STOPPING OF SWIFT PROTONS EVALUATED FROM STATISTICAL ATOMIC MODEL

BY

EJVIND BONDERUP

Synopsis

Calculations of electronic stopping for heavy particles with low charge number are performed down to quite low energies, e. g. for protons down to ~ 100 keV. The treatment is a refinement of a procedure suggested by LINDHARD and SCHARFF. This procedure makes extensive use of statistical models of the atom.

Stopping as a function of energy is determined by the I-value of the target material and the energy dependent "shell correction". As discussed, the shortcomings of the present statistical treatment should show up mainly in the I-values. In fact, the shell corrections obtained appear to be comparatively accurate, especially in view of the fact that previous estimates have been made by fitting parameters in semi-empirical formulas.

There is also a discussion of the possibility of determining I-values from theoretical shell correction curves and experimental stopping powers at very low energies.

§ 1. Introduction

The present paper will be concerned with electronic stopping of a heavy particle of low charge penetrating a substance with randomly distributed atoms. In such a situation quantal perturbation theory should be applicable down to quite low energies—e.g. for protons, which will be our standard projectiles, down to ~ 100 keV (cf. p. 10).

Although deflections in the screened atomic fields are of major importance in determining the scattering of the incoming particle, it is well known that the contribution to total stopping from these nuclear collisions can be neglected at the energies mentioned above[1].

§ 2. Review of Theory and Definition of Model

For electronic stopping one finds in a perturbation treatment that the specific energy loss, $(-dE/dx)_e$, suffered by a heavy incoming particle with charge $Z_1 e$, will be given by

$$(-dE/dx)_e = \frac{4\pi Z_1^2 e^4}{mv^2} N \cdot Z_2 L(v, Z_2), \tag{1}$$

m, v and N being, respectively, the electron mass, the velocity of particle 1 and the density of target atoms with atomic number Z_2. The dimensionless function $L(v, Z_2)$ is the one to be evaluated. The use of perturbation theory introduces the important simplification that the incoming particle appears in formula (1) only through the factor $(Z_1 e)^2$. Hence, the problem of evaluating the electronic stopping power is reduced to a treatment of the target material.

For v much larger than the velocities of the electrons in the stopping material $L(v, Z_2)$ is given by Bethe's expression

$$L(v, Z_2) = \sum_n f_n \log \frac{2mv^2}{\hbar \omega_n} + \log \frac{1}{1 - (v/c)^2} - \left(\frac{v}{c}\right)^2, \tag{2}$$

1*

the summation being performed over all possible transition frequencies ω_n with corresponding dipole oscillator strengths f_n ($\sum f_n = 1$). Relativistic terms enter only as the fourth and higher powers of v/c and are omitted in the following.

Before entering into actual calculations of $L(v, Z_2)$, let us briefly consider the possibility of applying similarity of the kind characteristic of the Thomas-Fermi description of the atom. The line of argument is the one given in refs. 2 and 3a.

In a dynamic Thomas-Fermi model f_n should only be a function of the one variable ω/Z_2, the frequency scale being proportional to Z_2. Moreover, denoting the dipole oscillator strength density by $g(\omega/Z_2)^*$ we get from (2) the asymptotic formula

$$L(v, Z_2) = \int_0^\infty g\left(\frac{\omega}{Z_2}\right) \log \frac{2mv^2}{\hbar Z_2(\omega/Z_2)} d\left(\frac{\omega}{Z_2}\right). \tag{3}$$

Here, L only depends on v and Z_2 in the combination v^2/Z_2. Thus, if we define a new energy measure x by[6, 2]

$$x = \frac{v^2}{v_0^2 Z_2} \quad (v_0 = e^2/\hbar), \tag{4}$$

L can be expressed as

$$L = \log x + \log \frac{2mv_0^2}{I_0} \tag{5}$$

with I_0 given by

$$\log I_0 = \int_0^\infty g\left(\frac{\omega}{Z_2}\right) \log \hbar\left(\frac{\omega}{Z_2}\right) d\left(\frac{\omega}{Z_2}\right). \tag{6}$$

In a real atom, the distribution of oscillator strength differs somewhat from that of a Thomas-Fermi model. At intermediate values of ω/Z_2 the departure from the smoothly decreasing function $g(\omega/Z_2)$ should reflect the presence of various electronic shells and thus be of an oscillating nature. However, a more systematic deviation is expected below a frequency $\omega \sim \omega_R$ ($\hbar\omega_R = mv_0^2/2$), ω_R giving e.g. the order of magnitude of both the ionization frequency of an inert gas and the plasma frequency of the valence electrons in a metal. This means that the integral representing $\log I_0$ will receive only

---

* An evaluation of $g(\omega/Z_2)$ from a hydrodynamical type of Thomas-Fermi model was suggested by Bloch in 1933[4] and has recently been carried through by Ball[5].

very small contributions below a value $(\omega/Z_2)_{\text{cut-off}}$. On the whole, $(\omega/Z_2)_{\text{cut-off}}$ is proportional to Z_2^{-1}, but significant individual fluctuations exist. Hence, $g(\omega/Z_2)$ being a decreasing function, departures from the Thomas-Fermi prediction for the I_0-value should arise mainly because of deviations of the oscillator strength distribution from $g(\omega/Z_2)$ at the low frequency end of the spectrum. This observation seems essential not only for the calculation of I_0-values, but also for any attempt to continue the evaluation of $L(v, Z_2)$ down to values of v where the asymptotic formula (2) does not apply. In fact, the contribution to L from the low frequencies must remain of order of $\sum f_n \log(2mv^2/\hbar\omega_n)$, and thus the effect being responsible for the most pronounced departure from a similarity description at high energies should persist down to quite low energies.

One way of handling the many body problem involved in calculating $L(v, Z_2)$ for all values of v and Z_2 would be to solve a system of self-consistent equations for the electromagnetic field inside the target material. However, a main difficulty of such a (microscopic) dielectric treatment of an atomic system arises from the fact that the electron density varies in space. In order to avoid this difficulty, LINDHARD and WINTHER[7] considered the idealized case of a free electron gas, which, as discussed in the following, provides a good starting-point for more realistic situations. Suppose that a Fermi gas is disturbed by a charge density $\varrho_0(\vec{r}, t)$ and that this gives rise to a potential $\Phi(\vec{r}, t)$. If the disturbance can be considered as a perturbation, a linear description can be applied, and all the information about the stopping material, necessary to calculate $L(v, Z_2)$, is contained in the longitudinal dielectric constant ε^l connecting the Fourier components $\varrho_0(\vec{k}, \omega)$ and $\Phi(\vec{k}, \omega)$ of ϱ_0 and Φ. In fact, defining $\varepsilon^l(\vec{k}, \omega)$ by the equation

$$k^2 \varepsilon^l(k, \omega) \Phi(\vec{k}, \omega) \equiv 4\pi\varrho_0(\vec{k}, \omega), \tag{7}$$

one has[7]

$$L = \frac{i}{\pi\omega_0^2} \int_0^\infty \frac{dk}{k} \int_{-kv}^{kv} \omega \left\{ \frac{1}{\varepsilon^l(k, \omega)} - 1 \right\} d\omega, \tag{8}$$

ω_0 and i being, respectively, the plasma frequency $\sqrt{4\pi e^2 N \cdot Z_2/m}$ and the imaginary unit. (Because of isotropy in coordinate space, ε^l does not depend on the direction of $\vec{k}$.) From the calculations in ref. 7 several important results have emerged, especially concerning the question of the effect on the oscillator strength distribution of the polarizability of the medium.

LINDHARD and SCHARFF[6, 2] argued that even if a dielectric calcula-
tion could not be carried through for the atomic case, the picture of a
polarizable electron gas should still be useful. One could try to average L
for a gas of constant density over the electron cloud of the atom, thus making
a statistical approach to the many body problem. However, some way or
other, the effect of the electrons not beeing free, should be introduced in the
expression for the stopping contribution from the various parts of the electron
cloud.

From such considerations it was suggested that

$$L = \frac{1}{Z_2} \int_{r_{min}}^{\infty} 4\pi r^2 \varrho(r) \log \frac{2mv^2}{\gamma \hbar \omega_0(r)} \, dr, \quad 2mv^2/\gamma \hbar \omega_0(r_{min}) = 1 \qquad (9)$$

could be expected to give a fair approximation even down to rather small
values of v. Here, $\varrho(r)$ is the electron density in an atom of the target material,
and $\omega_0(r)$ the corresponding local plasma frequency $\sqrt{4\pi e^2 \varrho(r)/m}$. For $\varrho(r)$
the densities found in for instance a Thomas-Fermi or a Hartree description
could be used. Qualitative arguments were presented[6] to show that the
binding forces acting on the electrons probably could be approximately
accounted for by the constant γ, appearing in (9). γ was expected to be of
order of $\sqrt{2}$. The values of I_0, calculated from (5) and (9), are seen to be-
come proportional to γ, and $\gamma = \sqrt{2}$ gives fair agreement with experimentally
determined mean excitation energies[2].

In the Lindhard-Scharff model a distinction was made between "outer"
electrons $(2mv^2/\sqrt{2}\hbar\omega_0(r) > 1)$, the contribution of which was calculated
as if at rest, and "inner" electrons $(2mv^2/\sqrt{2}\hbar\omega_0(r) < 1)$ that were considered
to give no stopping at all. With a cut-off of this kind, L remains a function
of x only, when the Thomas-Fermi expression for $\varrho(r)$ is used. If we compare
with (3), an essential aspect of (9) can be expressed in the following way:
L is supposed to be obtainable as an average of a function $L(\omega_0, v)$ weighted
with a dipole oscillator strength density for which an ansatz has been made.

The frequency $\sqrt{2}\omega_0$ should correspond to the density $-4\pi r^2 \varrho(r) \left. \dfrac{dr}{d\omega_0} \right|_{r=r(\omega_0)}$.

The results presented in ref. 2 were so promising, even down to energies
around maximum in stopping cross section, that it might be profitable to
repeat the calculations with the same ansatz for the oscillator strength
distribution, but with a refined expression for $L(r,v) \equiv L(\omega_0, v)|_{\omega_0 = \omega_0(r)}$.

In their treatment of a free electron gas, LINDHARD and WINTHER[7] showed that L can be expanded in powers of $(v_F/v)^2$, v_F being the velocity of an electron at the Fermi surface. It turned out that for a gas with plasma frequency ω_0 and average kinetic energy $\langle T \rangle$ the first correction term $(\Delta L)_1$ to the asymptotic formula

$$L = \log \frac{2mv^2}{\hbar\omega_0},\qquad(10)$$

was given by

$$(\Delta L)_1 = -\frac{\langle T \rangle}{mv^2/2}.\qquad(11)$$

Moreover, FANO and TURNER[3b] found this sort of expression to be of general validity in the atomic case (with $\langle T \rangle$ being the average over both coordinate and momentum space). As pointed out by LINDHARD and WINTHER[7], it would therefore seem natural to put

$$L(r,v) = \log\left(\frac{2mv^2}{\sqrt{2}\,\hbar\omega_0(r)}\right) - \frac{\langle T \rangle(r)}{mv^2/2}\qquad(12)$$

for the "outer" electrons. Here, the average kinetic energy $\langle T \rangle(r)$ of a unit volume at a distance r from the nucleus should, as always in a statistical description of the atom, be obtained from $\varrho(r)$ by means of the formula

$$\langle T \rangle(r) = \frac{3}{5}\frac{\hbar^2}{2m}(3\pi^2\varrho(r))^{2/3}.\qquad(13)$$

The behaviour of an electron gas is well described by a free particle model only at high densities[7], more specifically, when $\chi^2 \lesssim 1$, χ being defined by

$$\chi^2 = \frac{e^2}{\pi\hbar v_F}.\qquad(14)$$

The Lenz-Jensen model of the atom[8] shows that, when $Z_2 = 10$, $\chi^2(r)$ is less than 1 for 97 % of the electrons (v_F and thus χ now being functions of r), and for higher values of Z_2 the situation is even better. A typical order of magnitude in the electron cloud is $\chi^2(r) \sim 10^{-1} - 10^{-2}$.

Let us try to find a reasonable expression for the stopping contribution from the inner electrons of an atom. From the $(k, \omega/k)$-diagrams of ref. 7 (Figs. 1 and 3) it is seen that for sufficiently large v the decisive aspect is

that for $k \to \infty$ (close collisions with single electrons), and $k \to 0$ (distant collisions) the oscillator strength is contained in a strip around the line $\omega/k = \hbar k/2m$ and in a resonance curve corresponding to $\varepsilon^l(k, \omega) = 0$, respectively. The distribution for intermediate values of k is not important as long as all the oscillator strength corresponding to a fixed value of k can be assumed to be below the line $\omega/k = v$.

However, in case the velocity of the incoming particle is small compared to orbital velocities of atomic electrons, this situation is changed fundamentally. Now it will not be sufficient to know the distribution of oscillator strength in asymptotic limits, and the oscillator strength will not be collected in resonance curves (ref. 7, Fig. 1). On the one hand, it seems difficult to tell exactly how the distribution is shifted when free electrons are replaced by bound ones, but, on the other hand, there is no evidence of systematic shifts of the kind appearing for large v. The latter shifts, which correspond to changes in the resonance frequencies, should be accounted for by the introduction of the factor $\gamma \sim \sqrt{2}$ in (9). Furthermore, the contribution to total stopping from inner electrons is known to be small, cf. also § 3. We can therefore probably give a fair account of the slowing-down due to inner electrons by just taking over the expression for the stopping of a slow particle in a free electron gas. Thus, defining $\chi^2(r)$ as in (14), we put up the following formula for $L(r, v)$ (ref. 7, formulae (12) and (15)):

$$
L(r,v) = \begin{cases} \log\left(\dfrac{2mv^2}{\sqrt{2}\,\hbar\omega_0(r)}\right) - \dfrac{\langle T\rangle(r)}{mv^2/2}, & \text{if } \geq 0 \quad \text{(a)} \\[4mm] \left(\dfrac{\chi^2(r)}{3}\right)^{3/4}\dfrac{1}{2}\left[\log\left(\dfrac{1}{\chi^2(r)}\right) - 1\right]\left(\dfrac{2mv^2}{\hbar\omega_0(r)}\right)^{3/2} & \text{otherwise} \quad \text{(b)}. \end{cases}
\tag{15}
$$

Fig. 1 contains a reproduction of Fig. 5 in ref. 7, showing L as a function of $y = 2mv^2/\hbar\omega_0$ for two gas densities, $\chi^2 = 0.1$ and $\chi^2 = 0.01$. Here, the scale at the left-hand side should be used. The full drawn and dashed curves refer to numerical calculations and asymptotic expressions, respectively. With the scale to the right, the upper dashed and the dot-and-dash curves represent (a) and (b) of (15) at the same constant values of χ^2. It is noted that (b) is the result of an approximation which for high densities does not differ much from the one given in ref. 7, formula (15).

In connection with Fig. 1, two remarks should be made. First, the passage from (a) to (b) in (15) ought to occur at a value of r, where $\langle T\rangle(r) \sim 1/2\,mv^2$. This is seen to be fulfilled. Second, it would have been preferable
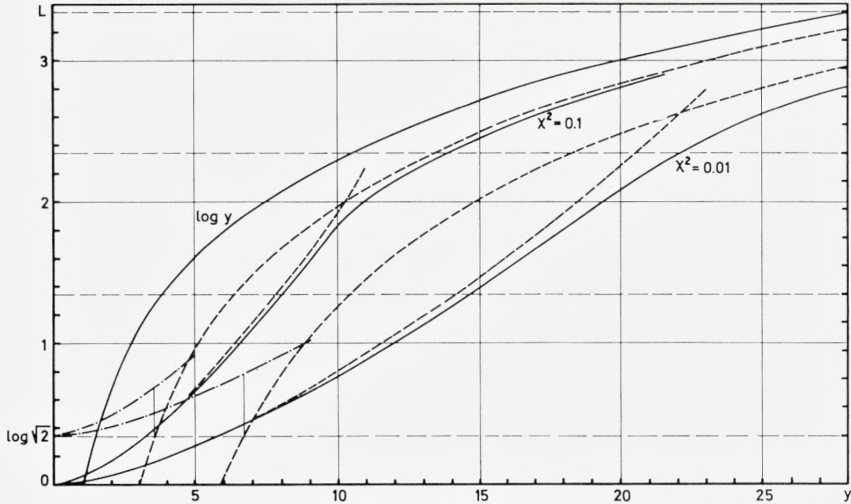
Figure 1. For explanation cf. text.

to avoid the discontinuity in $L(r, v)$, but it seemed difficult to find a simple analytic expression connecting (a) and (b) in a smooth manner. It will be shown later, however, that the discontinuity is of only little importance for the results of the calculations.

With $L(r, v)$ given by (15) the similarity as expressed by $L = L(x)$ is lost, even if $\varrho(r)$ is taken from a Thomas-Fermi model. However, as a function of (x, Z_2) the Z_2-dependence of L must still be only weak.

From the general discussion of oscillator strengths given at the beginning of this chapter it is to be expected that the detailed distribution of the outermost electrons is essential for the calculation of I_0-values. That this is so indeed, can be demonstrated by an example: Using a tabulated[9] Hartree-Fock distribution for $C(Z_2 = 6)$ I_0 was determined to 11.43 eV. By calculating the volume per atom in amorphous carbon it was found that 0.42 of the six electrons (7%) were situated outside this volume. Smearing out these 0.42 electrons equally over the accessible space, one altered I_0 to 13.75 eV – a change of 20%.

In order to avoid the large dependence of the calculated quantity on the details in the outermost part of the electron cloud, it was decided to look at the function C/Z_2 defined by

$$\left(-\frac{dE}{dx}\right)_e = \frac{4\pi Z_1^2 e^4}{mv^2} N \cdot Z_2 \left\{\log\left(\frac{2mv^2}{I}\right) - \frac{C(x, Z_2)}{Z_2}\right\} \quad (I = I_0 \cdot Z_2) \quad (16)$$

rather than at $L(x, Z_2)$. This seems to be the most direct way of comparing with experiments and thereby obtaining information about the applicability of the Lindhard-Scharff ideas to such detailed calculations.

The conventional term "shell correction" for C/Z_2 is somewhat misleading in the present treatment, but will be used, nevertheless.

Before making comparisons with experimental material one question should be considered. The present procedure rests upon the outcome of a perturbation calculation for a free electron gas. To what extent can a perturbation treatment be used in our case? The electron cloud was divided into two parts: a) "outer" electrons corresponding to $v \gtrsim v_F(r)$, and b) "inner" electrons corresponding to $v \lesssim v_F(r)$. Case a) should be tractable by (quantum mechanical) perturbation theory for $\varkappa > 1$, where[3a, 10]

$$\varkappa \equiv \frac{2Z_1 e^2}{\hbar v}, \tag{17}$$

and for case b) a perturbation calculation can be shown to be valid for comparatively high gas densities—more specifically, if $v_0 \cdot Z_1^{2/3} \lesssim v_F(r)$ (LINDHARD). For protons, the two requirements are satisfied for $v \gtrsim 2v_0$, i.e. for energies down to ~ 100 keV. Although depending on the target material, 100 keV gives the order of magnitude for the energy at which the maximum in stopping power appears.

It might be mentioned that calculations for proton energies below ~ 500 keV have often been considered to be doubtful due to capture and loss of electrons. However, within a self-consistent dielectric treatment of a Fermi gas the electrons provide a time-independent screening of an incoming positive particle, the screening distance being generally a function of Z_1, v and the density of the gas. Therefore, such a description includes a balance between capture and loss. The special case of a linear treatment corresponds to the situation where the screening distance does not depend on Z_1.

We now seem justified in comparing theoretical and experimental data down to $x \sim 10^{-1}$, at least for the heavier elements.

§ 3. Discussion of Results

Shell corrections and I-values

Let us now turn to the C/Z_2-curves that have been calculated by means of the procedure described above*. In Fig. 2 comparison is made between

---

* The Lenz-Jensen calculations were performed on the GIER computer at the University of Aarhus. As for the Hartree curves, the calculations were done by hand, but were much reduced through the use of unpublished numerical results from the original work by LINDHARD and SCHARFF.
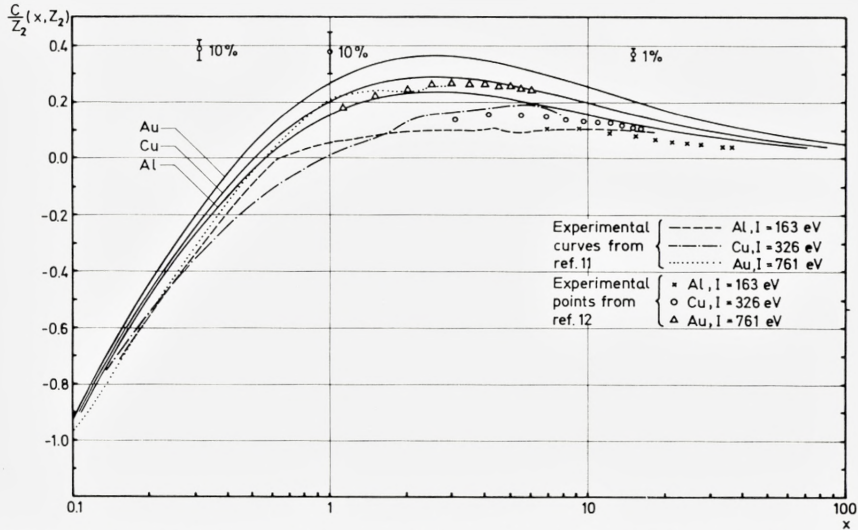
Figure 2. Comparison of experimental and theoretical shell corrections. The solid curves represent calculated values. The error bars show the approximate influence of a 10 % (1 %) uncertainty in the applied stopping power.

experimentally determined and computed shell corrections, the latter having been obtained by applying a Thomas-Fermi type of expression for $\varrho(r)$, namely the analytic first order Lenz-Jensen distribution function. The empirical curves were drawn by introducing experimental values for $(-dE/dx)_e$[11, 12] and I into (16), the I-values being those recommended in ref. 3 (I and not I_{adj} of ref. 3 should be used).

Two features are seen to be reproduced correctly by the computed shell corrections:

1) the general shape of the curves,
2) the order of magnitude of C/Z_2.

Furthermore, it seems to be in agreement with experiments that C/Z_2 should increase with increasing Z_2 (Fig. 2 and ref. 3c). However, a detailed check on this point is difficult because of the significant experimental uncertainties, especially as regards the I-values (cf. below).

Low energies

Although the difference between the calculated shell corrections for Al and Au, taken relatively to L, i.e. $\Delta(C/Z_2)/L$, amounts to about the same
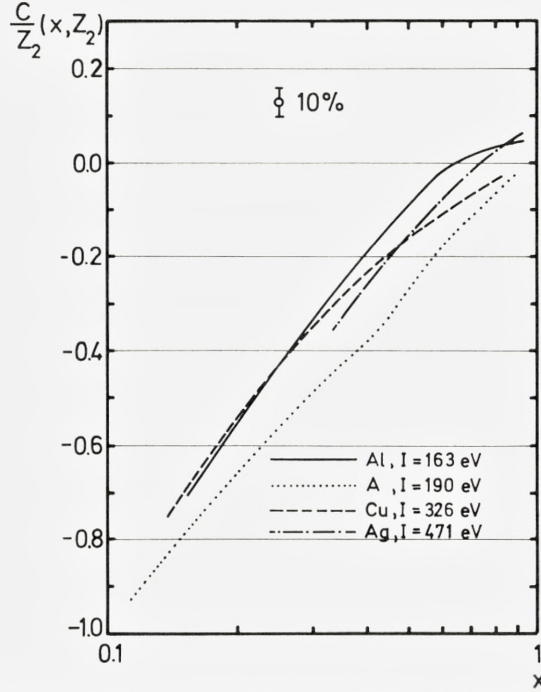
Figure 3. Shell correction curves determined from Bichsel's stopping power data and experimental I-values. The error bar shows the approximate influence of a 10 % uncertainty in the applied stopping power.

at $x = 0.1$ and $x = 1$ (8–10%), the small difference on an absolute scale between the various C/Z_2-curves at low energies seems to be of some importance. Suppose that one wants to extract the I-value of a material from some experimentally determined stopping power and a theoretical value for the corresponding shell correction. The formula to be used is

$$L(x, Z_2)_{\text{exp}} = \log x + \log\left(\frac{2mv_0^2}{I/Z_2}\right) - \frac{C}{Z_2}(x, Z_2), \qquad (18)$$

where $L(x, Z_2)_{\text{exp}}$ is found by means of (1) in an obvious way.

If L has been measured with an uncertainty ΔL and C/Z_2 is given with an error $\Delta(C/Z_2)$ one has for the maximum possible error ΔI in I:

$$\frac{\Delta I}{I} \simeq -\left[\left(\frac{\Delta L}{L}\right) \cdot L + \Delta\left(\frac{C}{Z_2}\right)\right]. \qquad (19)$$

In a high energy experiment L is of order of 6–10. However, at $x = 0.1$ the L-value will be at most 0.5, which means that an uncertainty of 10% in the measured stopping power leads to an experimental uncertainty in I of only 5%. If C/Z_2 can be calculated in such a way that $\Delta(C/Z_2) \lesssim 0.10$, say, the extracted I-value will be determined with a total uncertainty not exceeding 15%.

Admittedly, it is most pronounced for the theoretical shell corrections that the curves approach each other at low x-values (Figs. 2 and 3). Yet, it must be remembered that, firstly, the stated uncertainty of $1–10\%$ in the stopping powers reported by BICHSEL[11] is of some importance for the drawing of the empirical curves, and, secondly, a change of 1% in the applied experimental I causes a parallel shift of the corresponding curve of 0.01. Therefore, even if it is true that the shell correction depends in an only weak manner on Z_2 at small x-values, it would probably be very difficult to point out such an effect from existing experimental material alone, i.e. from stopping power data at low energies and I-values determined at high energies.

TABLE 1.

Lenz-Jensen calculation for Ag. Z_2^*: number of "inner electrons". L^*: contribution to L from "inner electrons".

x	Z_2^*/Z_2	L^*	L^*/L
8.04	0.07	0.014	0.00
3.62	0.16	0.028	0.01
1.055	0.40	0.054	0.04
0.613	0.52	0.058	0.06
0.376	0.63	0.059	0.08
0.235	0.72	0.055	0.10
0.095	0.85	0.038	0.14

Before giving any examples of I-values obtained along the lines suggested above, let us make a couple of further remarks concerning the reliability of the method used for calculating shell corrections. One difficulty might seem to be that a large portion of the electron cloud is considered as belonging to "inner" electrons at small x-values, and the contribution from an inner electron was only taken care of through a rough estimate. This problem is, however, not very serious because, as shown in Table 1, the role played by these electrons in the slowing-down is very limited, both relatively and
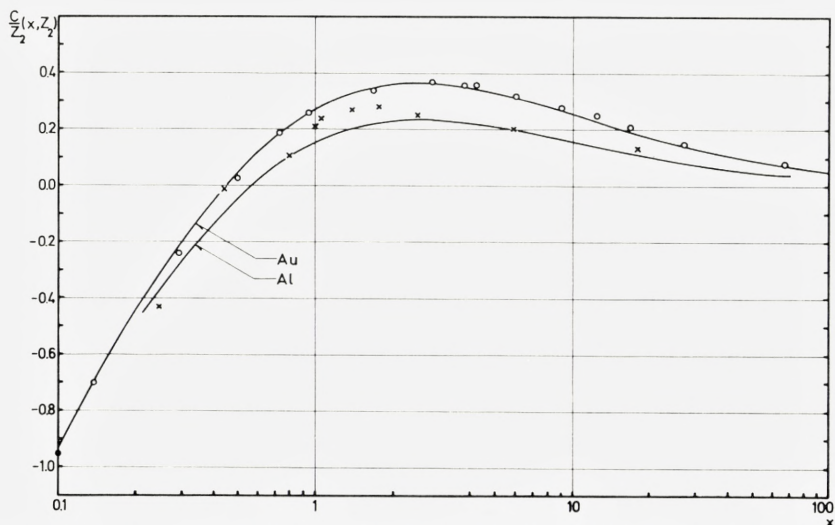
Figure 4. Solid curves represent results from Lenz-Jensen calculations. Points from corresponding Hartree models are denoted by x (Al) and o (Au).

absolutely. Moreover, Table 1 makes it very plausible that the discontinuity in the expression for $L(r, v)$ cannot be of much importance. As a matter of fact, an estimate shows that by changing $L(r, v)$ in such a way that (a) and (b) in (15) become smoothly connected, one changes C/Z_2 by less than 0.01–0.02.

The calculated shell corrections should thus depend only weakly on the detailed distribution of both inner and outermost electrons, but this is, in fact, what justifies the use of a statistical method. Especially the introduction of Hartree models for the electron clouds should for heavier materials only lead to slight deviations (oscillations) from the Lenz-Jensen results (Fig. 4).

If a common C/Z_2-curve can be drawn in a certain x-interval for two materials denoted by indices A and B, the corresponding L-values will only differ by a constant reflecting the difference in I for the two substances. More specifically, the following relation should apply:

$$I_A = I_B \frac{Z_A}{Z_B} \exp(L_B - L_A). \tag{20}$$

To test formula (20) it was decided to take Al as a standard, because this material seems to be the one with the experimentally best known I. A value

TABLE 2.

Comparison of calculated and empirical I-values. In several cases ref. 3 only gives I_{adj}. $(I_{adj} - I)$ was then found by interpolation in the table on p. 101 of the same publication. BICHSEL does not consider his value for Ag to be reliable. FANO has taken his value for Kr from BICHSEL.

Element	Z_2	x	I_{cal}(eV)	I_{exp}(eV) FANO	I_{exp}(eV) BICHSEL	I_{exp}(eV) BARKAS & BERGER	$\exp(L_B - L_A)$
C	6	0.667	70± 8	81		78	0.925
Ne	10	0.400	144 ± 9			131	1.146
A	18	0.308	157 ±15	190	184 212	210	0.696
Ni	28	0.308	296 ± 23		307.5 310	302	0.844
Cu	29	0.308	319 ±23	313	326	312	0.878
Kr	36	0.308	355 ± 30	360	360 380	377	0.787
Ag	47	0.340	433 ± 42	471	447.5	480	0.736
Sn	50	0.320	460 ± 43			507	0.733
Xe	54	0.308	462 ±45			543	0.683
Au	79	0.308	779 ± 66	761		768	0.787
Pb	82	0.308	769 ± 69	788		795	0.748

of 163 eV was taken from ref. 3. The stopping power measurements used for the determination of L were those cited by BICHSEL[11], the x-value always being the lowest one common to Al and the medium under consideration. However, measurements below 100 keV were not taken into account.

Table 2 shows the results from such a calculation (I_{cal}) together with empirical I-values. The uncertainty in I_{cal} corresponds to the stated maximum experimental error in the stopping power for the substance investigated (10%). As already mentioned, the experimental I-values are often uncertain, a fact clearly demonstrated by the different numbers given for the same material by the authors of ref. 3.

For an account of how the experimental mean excitation energies were found, the reader is referred to ref. 3. Here, we merely note that the numbers given by BARKAS and BERGER[3d] for $Z_2 \geq 13$ were determined by means of a semi-empirical formula for I/Z_2, giving very closely the values quoted by FANO[3c] for Al, Cu, and Pb. Yet, in some cases, e.g. for the noble gases, an interpolation procedure of this kind may not be very reliable, since the distribution of the outermost electrons can be rather special. The last column
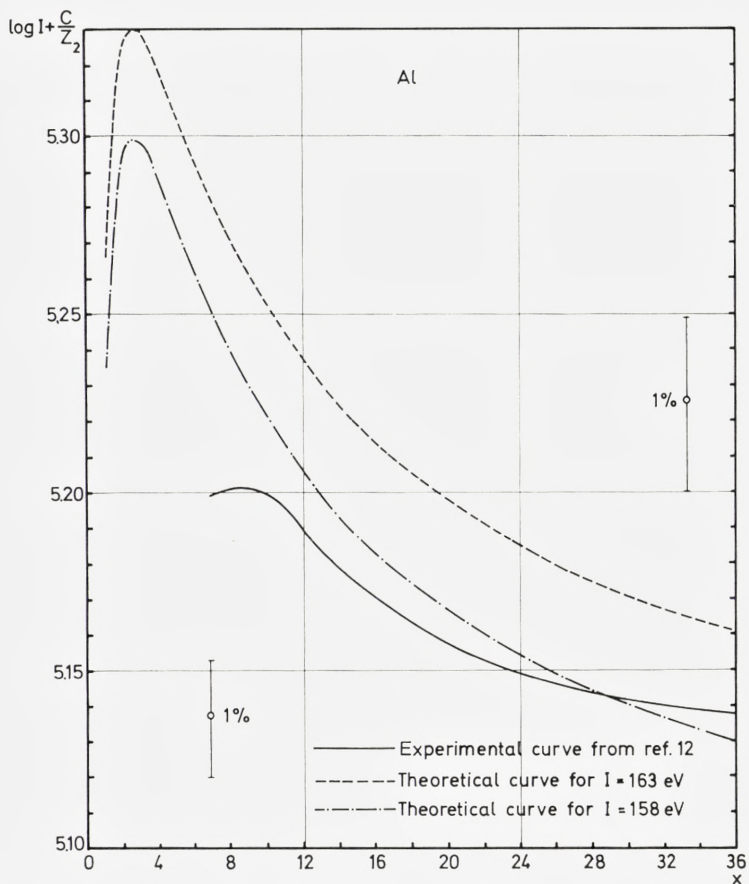
Figure 5a. The error bars show the influence of a 1 % change in the experimental stopping power (similar for Fig. 5b).

of Table 2 exhibits the factors $\exp(L_B - L_A)$ reflecting the rather large variations of I/Z_2.

The agreement with the I-values suggested in ref. 3 is rather good considering the experimental uncertainties. It seems that these have not been exaggerated by the authors. For instance, the stopping powers for protons in carbon measured recently by SAUTTER and ZIMMERMANN[13] with a reported accuracy of $\pm 1.7 - \pm 2.3 \%$, are lying from 11.4% to 15.5% below Bichsel's values in the region of overlap (100–300 keV).

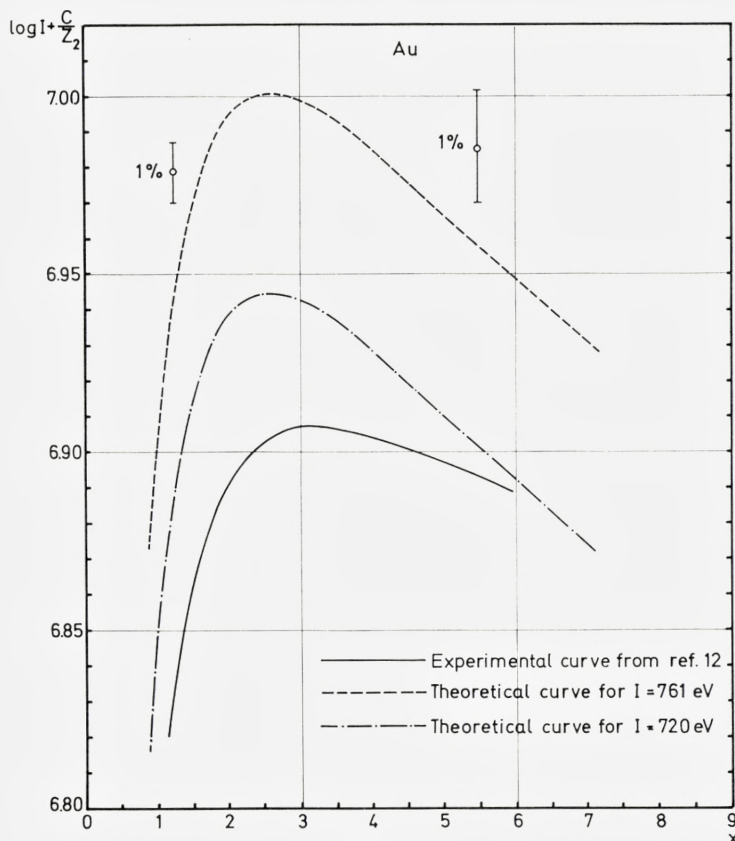From the theoretical curves C/Z_2 was found to increase for increasing Z_2.

Figure 5 b.

Thus, choosing an experimental shell correction curve for Al as a common standard for all materials, one should for $Z_2 > 13$ have underestimated C/Z_2 and thereby overestimated I, this being the more serious the larger the used x. However, in Table 2 the calculated I-values are not systematically larger than the corresponding experimental ones. Yet, although $I_{exp} = 163$ eV for Al may be determined with considerable accuracy, the stopping power measurements at low energies are probably not much better for Al than for most other metals. In this context it may be noted that a 10% change in the stopping power for Al at $x = 0.308$ ($E_{proton} = 100$ keV) would correspond to a systematic change in the calculated I-values of $\pm 6\%$.

Intermediate energies

The above discussion of the region of small x-values originated in a general feature of the calculated shell corrections. A direct comparison between theory and experiments appeared to be difficult.

At intermediate energies the experimental situation is much more satisfying, mainly due to a new technique for measuring stopping powers developed by ANDERSEN, GARFINKEL, HANKE, SØRENSEN, and VAJDA[12]. According to these authors, the data obtained are reliable to within $\pm 0.3\,^0/_0$. This means that a detailed comparison between, at least, the shapes of the experimental and theoretical shell correction curves can be made for the energies investigated (2–12 MeV protons).

Figs. 5 a and 5 b show a plot of $\log I + C/Z_2$ against x for Al and Au. For both elements, the second I-value used for the calculated curve has been chosen to avoid a parallel shift between corresponding theoretical and empirical curves rather than being in close agreement with current estimates. It is seen that the location of the maximum is accounted for fairly well, but there is a significant difference in the trend towards it, the calculated curves being much too steep.

It is not at all evident if this discrepancy can be removed within the model by some appropriate change, but it might be in place to note that the x-values in question correspond to the "bulk" of electrons passing from being counted as "outer" to being counted as "inner" electrons, i.e. the maximum of the function $4\pi r^2 \varrho(r)$ appears around the radius where one goes from (a) to (b) in (15).

§ 4. Concluding Remarks

The purpose of the present paper may be said to have been twofold. Firstly, from a theoretical point of view it seemed desirable to investigate the applicability of the Lindhard-Scharff ideas in a detailed evaluation of slowing-down problems, and, secondly, even if the results of the calculations should not be in very accurate quantitative agreement with experiments, it might well be that such a treatment of Thomas-Fermi type could give some information as to the over all dependence of fundamental quantities on the atomic number Z_2. As discussed, such information is not always easy to extract from experimental material alone.

Keeping in mind the detailed nature of any theoretical description trying to account for shell corrections, the results obtained must be interpreted as supporting the basic assumptions of the method. Furthermore, the expression
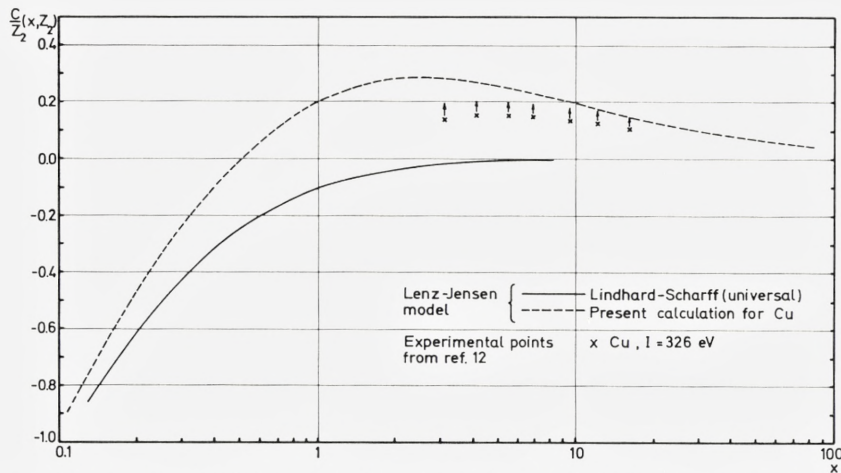
Figure 6. Comparison of Lindhard-Scharff model with present calculations. Arrows at experimental points correspond to a change of I from 326 eV to 312 eV (cf. Table 2).

chosen for $L(r, v)$ probably cannot be much in error. An indication of this is provided by a comparison of the present shell corrections with the (universal) Lenz-Jensen curve from the model used by LINDHARD and SCHARFF (Fig. 6).

Acknowledgments

References

1. J. LINDHARD, M. SCHARFF, and H. E. SCHIØTT, Mat. Fys. Medd. Dan. Vid. Selsk. **33**, no. 14 (1963).
2. J. LINDHARD and M. SCHARFF, Report on Conference on Penetration of Atomic Particles, Gatlinburg 1958. NAS-NRC Publ. 752 (1960).
3. Studies in Penetration of Charged Particles in Matter, NAS-NRC Publ. 1133 (1964).
3a. J. LINDHARD, paper no. 1 of ref. 3.
3b. U. FANO and J. E. TURNER, paper no. 4 of ref. 3.
3c. U. FANO, Appendix A of ref. 3 and Ann. Rev. Nucl. Sci. **13**, 1 (1963).
3d. W. H. BARKAS and M. J. BERGER, paper no. 7 of ref. 3.
4. F. BLOCH, Z. f. Physik **81**, 363 (1933).
5. J. A. BALL, unpublished thesis, Princeton University (1963).
6. J. LINDHARD and M. SCHARFF, Mat. Fys. Medd. Dan. Vid. Selsk. **27**, no. 15 (1953).
7. J. LINDHARD and AA. WINTHER, Mat. Fys. Medd. Dan. Vid. Selsk. **34**, no. 4 (1964).
8. H. JENSEN, Z. f. Physik **77**, 722 (1932).
9. A. JUCYS, Proc. Roy. Soc. London **173**, 59 (1939).
10. N. BOHR, Mat. Fys. Medd. Dan. Vid. Selsk. **18**, no. 8 (1948).
11. H. BICHSEL, American Institute of Physics Handbook, 2nd. ed., Sect. 8c (McGraw-Hill, New York 1963).
12. H. H. ANDERSEN, Risö Report No. 93 (1965); H. H. ANDERSEN, A. F. GARFINKEL, C. C. HANKE, and H. SØRENSEN, Mat. Fys. Medd. Dan. Vid. Selsk. **35**, no. 4 (1966); H. H. ANDERSEN, C. C. HANKE, H. SØRENSEN, and P. VAJDA, Phys. Rev. **153**, 338 (1967).
13. C. A. SAUTTER and E. J. ZIMMERMANN, Phys. Rev. **140**, A490 (1965).